doi:10.1016/j.jmb.2005.01.006 J. Mol. Biol. (2005) 347, 41–52

JMB

Available online at www.sciencedirect.com

SCIENCE DIRECT®

ELSEVIER

Atomic Force Microscopy Analysis of Icosahedral Virus RNA

Yurii G. Kuznetsov[1], Sarah Daijogo[2], Jiashu Zhou[1], Bert L. Semler[2] and A. McPherson[1]*

[1]*Department of Molecular Biology and Biochemistry University of California, Irvine CA 92697, USA*

[2]*Department of Microbiology and Molecular Genetics University of California, Irvine CA 92697, USA*

**Corresponding author*

Single-stranded genomic RNAs from four icosahedral viruses (poliovirus, turnip yellow mosaic virus (TYMV), brome mosaic virus (BMV), and satellite tobacco mosaic virus (STMV)) along with the RNA from the helical tobacco mosaic virus (TMV) were extracted using phenol/chloroform. The RNAs were imaged using atomic force microscopy (AFM) under dynamic conditions in which the RNA was observed to unfold. RNAs from the four icosahedral viruses initially exhibited highly condensed, uniform spherical shapes with diameters consistent with those expected from the interiors of their respective capsids. Upon incubation at 26 °C, poliovirus RNA gradually transformed into chains of globular domains having the appearance of thick, irregularly segmented fibers. These ultimately unwound further to reveal segmented portions of the fibers connected by single strands of RNA of 0.5–1 nm thickness. Virtually the same transformations were shown by TYMV and BMV RNA, and with heating, the RNA from STMV. Upon cooling, the chains of domains of poliovirus RNA and STMV RNA condensed and re-formed their original spherical shapes. TMV RNAs initially appeared as single-stranded threads of 0.5–1.0 nm diameter but took on the structure of the multidomain chains upon further incubation at room temperature. These ultimately condensed into short, thick chains of larger domains. Our observations suggest that classical extraction of RNA from icosahedral virions produces little effect on overall conformation. As tertiary structure is lost however, it is evident that secondary structural elements are arranged in a sequential, linear fashion along the polynucleotide chain. At least in the case of poliovirus and STMV, the process of tertiary structure re-formation from the linear chain of secondary structural domains proceeds in the absence of protein. RNA base sequence, therefore, may be sufficient to encode the conformation of the encapsidated RNA even in the absence of coat proteins.

Keywords: RNA; conformation; encapsidation; structure; folding domains

Introduction

There is evidence from spectroscopy and biochemical modification experiments that a substantial amount of the RNA in small icosahedral viruses, perhaps 40% to 60%, resides in base-paired, helical segments.[1–4] This is indicated as well by analyses of viral RNAs in terms of probable secondary structure arrangements.[5,6] X-ray crystallographic analyses of some viruses from both plants and insects have demonstrated the presence of helical RNA within capsids.[1,7] In those cases, only the RNA elements that were consistent with icosahedral symmetry could be visualized; hence, it is likely that these were underestimates of all that might be present. Even so, in satellite tobacco mosaic virus (STMV), for example, about 45% of the RNA is seen to form double-helical elements,[4,8,9] in bean pod mottle virus about 20% exists in trefoil arrangements,[10] in turnip yellow mosaic virus (TYMV) roughly 40% is helical,[11] and in Flock house virus around 20%.[12]

From X-ray crystallography studies, the RNA molecules in both STMV and TYMV appear to be

Abbreviations used: TYMV, turnip yellow mosaic virus; BMV, brome mosaic virus; STMV, satellite tobacco mosaic virus; AFM, atomic force microscopy.

E-mail address of the corresponding author: amcphers@uci.edu

sequences of double-helical stem-loop substructures that are arranged in a linear manner. In the case of STMV, these occur at icosahedral 2-fold axes.[4,8,9] Such locations are particularly propitious, because helical RNA segments have dyads perpendicular to their helix axis and can, therefore, maintain consistency with the icosahedral symmetry of the virion. There is evidence that the RNA in other small icosahedral viruses may be arranged as linear sequences of stem-loop clusters distributed among the capsomeres with approximate icosahedral symmetry.[1,7] RNA regularity is, presumably, a consequence of its interaction with the symmetrically organized coat proteins.

Inspection of possible base-pairing arrangements in specific viral RNAs shows that there can be no exact periodicity to the occurrence of helical segments, nor could they be consistently of the same length or form perfect helices. Nonetheless, an imperfect, only approximately regular series of such segments could assume quasi-icosahedral symmetry. This would explain the appearance of icosahedrally ordered RNA helical segments in electron density maps derived by X-ray crystallography.

We have undertaken a study, using atomic force microscopy (AFM),[13,14] of the appearance of encapsidated RNA isolated from five different viruses, and their structural transformations. The five viruses whose RNA we extracted and visualized are poliovirus,[15–17] TYMV,[18–20] brome mosaic virus (BMV),[21–23] STMV,[3,4,24–27] which are all icosahedral viruses, and tobacco mosaic virus (TMV),[28–31] which is a helical, rod-shaped virus. We included TMV because its RNA molecules do not share the secondary or tertiary structural requirements of those of the icosahedral viruses.

The three-dimensional structures of all of the viruses investigated here have been solved by X-ray crystallography and characterized thoroughly both biochemically and biophysically. Their individual properties are presented in Table 1. It should be noted that STMV is a satellite virus that cannot replicate in the absence of its helper virus TMV, and that BMV has a multipartite genome with four different RNA molecules encapsidated.

The structure of viral RNA must be fluid and amenable to structural transformations, otherwise the mass of RNA within a virion could not undergo the many physiological processes involved in the viral life-cycle such as movement between cells, RNA replication and translation on ribosomes.[7,33,34] It must be strictly single-stranded under some conditions and highly self-involved under others. Thus, it may be expected that upon decapsidation or extraction, the RNA will undergo structural alterations that reveal something of its conformation in the folded state.[33,34]

Table 1. Properties of the viruses investigated by AFM

	Icosahedral *T* no.	Diameter (Å)	No. capsid subunit, mass (Da)	Genome length (nt)	Genome mass (Da)	Host	Genus	Crystallographic structure references	Review of properties references
TYMV	3	242–318	180/20, 133	6318	2.1×10^6	Chinese cabbage	Tymovirus	19	20,28
BMV	3	280	180/20, 346	3200	1.1×10^6	Millet	Bromovirus	23	21,22
				2800	9.34×10^5				
				2100	7.01×10^5				
				800	2.67×10^5				
STMV	1	166	60/17, 500	1058	3.5×10^5	Tobacco	Satellite virus	7,8	26,27
Poliovirus	p3	306–328	VP1-300	~7500	2.48×10^6	Human	Picornavirus	32	15–17
			VP2-238						
			VP3-271						
			VP4-69						
TMV	Helical (cylindrical)	$r=90$ $l=3000$	(2140)/17, 420	6394	2.1×10^6	Tobacco	Tobamovirus	29,30	2,31

Results

Four different RNA molecules extracted by

phenol/chloroform from icosahedral viruses, along with an RNA from a helical rod-shaped virus, were investigated by AFM. The icosahedral viruses were poliovirus, an animal virus, and the plant viruses TYMV, BMV, STMV, and TMV, a rod-shaped virus. Poliovirus, BMV and TYMV are $T=3$ icosahedral viruses, and STMV is a $T=1$ icosahedral virus.[35] Poliovirus has a genome length of approx. 7500 nucleotides (including a 3′ poly(A) tract of heterogeneous length),[36] TYMV 6318,[18] and STMV encapsidates 1158 nucleotides.[26] BMV is multipartite and encapsidates three principal RNA molecules of 3200, 2800, and 2100 nucleotides,[22] along with the last and smallest RNA, a subgenomic fragment of 800 nucleotides which is also encapsidated.[37,38] TMV has an RNA genome length of 6394 nucleotides,[29,30] which would have an extended length of 3.78 μm, assuming an average phosphate-to-phosphate distance of 6 Å. One would expect proportionate, extended lengths for the other RNAs.

Poliovirus RNA

Following extraction, the RNA was maintained frozen at −70 °C until thawed and then spread on treated mica and imaged by AFM in air. Immediately upon thawing, the RNA was seen to have the appearance, illustrated in Figure 1(a) and (b), of compact spheres of uniform size, and diameter about 30 nm. The diameter corresponds to the inside diameter of the poliovirus capsid, and is consistent with the condensed conformation of the encapsidated RNA.

After 30 minutes to an hour at 26 °C, or upon heating to 65 °C for one minute, the spherical particles of poliovirus RNA unravel, as seen in Figure 1(c) and (d), and assume a different three-dimensional conformation, that of an irregular, banded fiber, or chain of discrete densities. The chains of densities, having lengths of the order of 500 nm, are not smooth and uniform, but are segmented. They consist of small domains, presumably individual secondary structural elements, or groups of these, distributed in a linear manner. The thickness varies arbitrarily along the chains from only 0.5 nm to 3 nm or more. After incubation for one hour at 26 °C, virtually all of the spherical RNA particles unfold into these linear

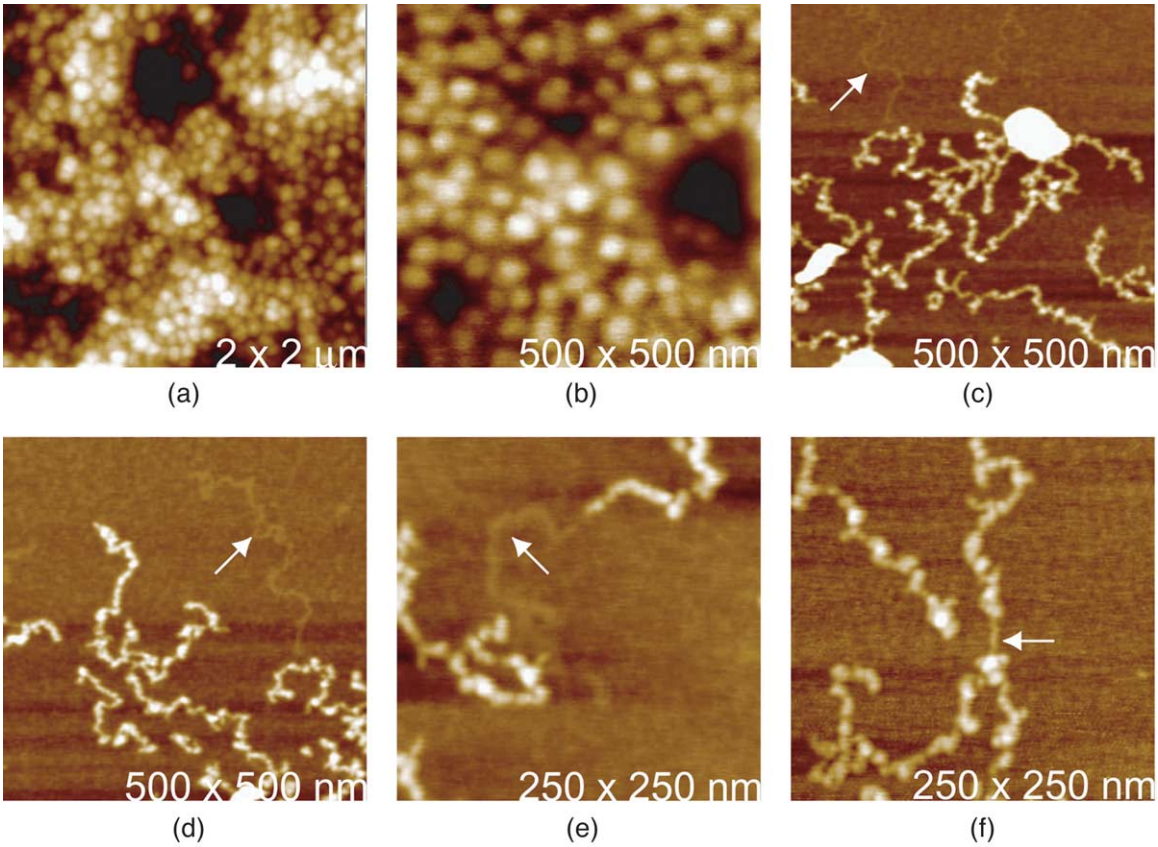

Figure 1. In (a), and at higher magnification in (b), is genomic RNA extracted from poliovirus using phenol/chloroform, which was thawed after freezing and immediately imaged by AFM after spreading on treated mica. Imaging was carried out at 26 °C in air. The RNA exists as uniform compact spheres of about 30 nm diameter, the interior diameter of the virion. With time, at 26 °C, the compact spheres of poliovirus RNA transform into the extended chains of structural domains seen in (c) and (d). In (d) a segment of an unwound strand of RNA appears and is marked by an arrow. The very high, white objects in (c) are RNA spheres that have not yet fully transformed into strands. In some higher magnification images of the poliovirus RNA, like those shown in (e) and (f), segments of the chains of structural domains can be seen joined to others by brief intervals of completely unwound, single-stranded RNA. These connecting links are indicated by arrows.

arrangements of structural domains, and the tertiary structure of the encapsidated RNA is lost.

Upon more prolonged incubation at 26 °C, the viral RNA opens further, domains melt, and longer stretches of single-stranded RNA having a height above the substrate of only 0.5 nm to 1 nm, become visible. Occasionally, entire RNA strands unwind, lose their secondary structure, and appear as long, single-stranded threads. In other cases, illustrated in Figure 1(e) and (f), sequences of secondary structural domains remain and are linked along a chain by single-stranded regions of RNA. If the RNA samples are heated to 65 °C or higher, which promotes further loss of base-pairing, then only single-stranded threads are visible, and these subsequently degrade to fragments.

Significantly, if the chains of secondary structural domains joined by single-stranded RNA, like those in Figure 1(c) through (f), are returned to cold temperature and then re-examined as before by AFM, then the original spheres of uniform diameter, ~30 nm, of Figure 1(a) and (b) are seen once again. Thus, the unfolding process is reversible and the RNA can re-establish its tertiary interactions and return to the globular state. The transformations between spheres and extended chains can be repeated indefinitely.

TYMV RNA

The structural transitions observed with TYMV RNA are very similar to those observed with poliovirus RNA. Freshly prepared, or frozen and thawed RNA initially appears as uniform spherical particles approximately the diameter of the inside of the virion (~20 nm). The spherical aggregates are, however, relatively stable at 26 °C. After 30 minutes to an hour at 40 °C, the spherical particles lose their integrity and assume an irregular banded fiber appearance, again segmented into secondary structural domains, and closely similar to those derived from poliovirus RNA. Examples are seen in Figure 2(a) and (b). Further heating to 65 °C for 15 to 20 minutes produces regions of single-stranded RNA connecting secondary structural domains, again similar to the RNA from poliovirus. Heating to higher temperature results in single-stranded threads followed by degradation to small fragments.

BMV RNA

The progression of events with BMV was similar to that for poliovirus and TYMV in most ways, but BMV RNA exhibited some distinctive differences. Initial images of RNA from freshly prepared virus again showed the presence of spherical particles having diameters consistent with virion interiors. Upon standing, or under heating, the spherical particles disappeared. However, chains of closely linked domains, the segmented fibers, were not evident. The substrate instead contained many small globules of approximately 1 nm in height, perhaps small folded fragments of RNA. In addition, as shown in Figure 2(c) and (d), some long, single-strands of RNA were observed, and

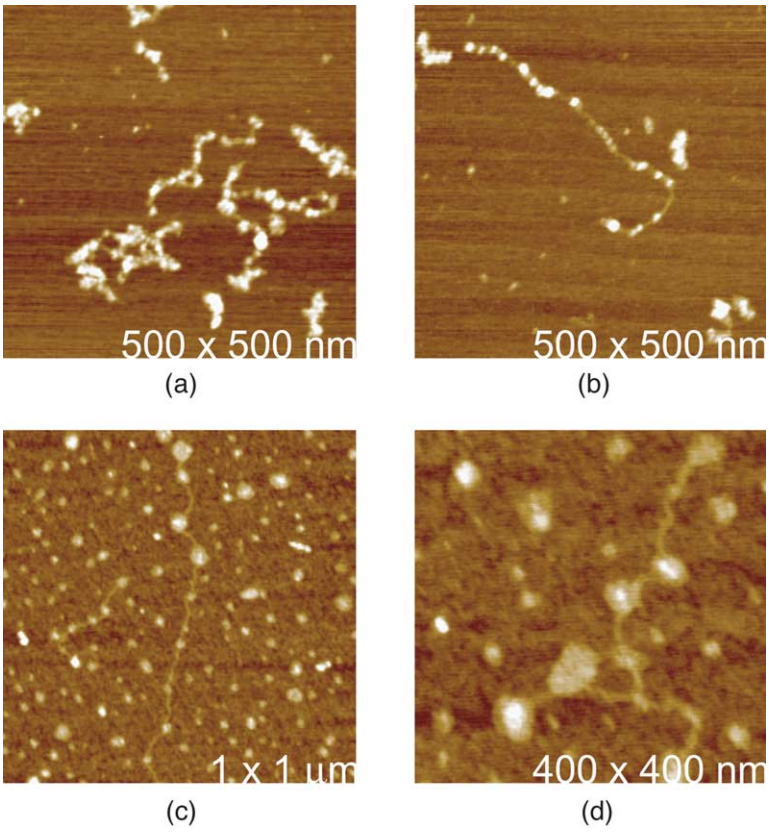

Figure 2. In (a) and (b) are RNA molecules extracted from TYMV that appear, in a manner similar to the RNA of poliovirus, as extended, linear chains of structural domains. (c) and (d) AFM images of RNA extracted from BMV, which tends to degrade and fragment readily. Single-stranded RNA containing some structural domains are nonetheless visible. In (d) the apparent branching of the RNA must be a consequence of two strands intersecting.

frequently these had, along their length, larger globular units, presumably representing locally folded single-stranded RNA.

There are two plausible explanations for our failure to observe linear chains of domains as we did for poliovirus and TYMV. One is that the chains were in fact produced from the spherical RNA, but failed to adhere to the substrate. However, this is not what we observed for the other four viruses and there is no additional evidence in support. The second explanation, which we favor, is that the BMV RNA contains significantly less helical structure, is more sensitive to hydrolysis, and may degrade quickly to small compact fragments.

In Figure 2(d) we observed an apparent branching of the RNA, a unique feature not observed in any other preparations of RNA. All branches appear to be single-stranded. We conclude that this RNA form must represent two separate nucleic acid strands. Such a possibility is likely, given the multipartite nature of BMV and the fact that some particles contain two different RNA molecules.[22,38]

STMV RNA

The RNA from STMV was the most difficult to investigate because of the exceptional stability of the virion, and the equally stable structure of its encapsidated RNA. Nevertheless, a similar progression of states was produced, but only by application of more rigorous denaturing conditions. As seen in Figure 3(a) and (b), upon initial extraction with phenol/chloroform, either preceded by digestion with proteinase K or not, the RNA appears as uniform spherical particles having diameters of 10 nm. These RNA cores of STMV were previously characterized by light-scattering and visualized by AFM,[39] and they can, in fact, be produced by exposure of virions to the protease alone during incubation at 65 °C for 30–40 minutes. Thus, they are not unique to material extracted with phenol/chloroform. The diameter of 10 nm corresponds to the interior cavity of STMV virions and, as in poliovirus, TYMV and BMV, corresponds to the approximate size and shape of the encapsidated RNA. The spherical STMV RNA particles,

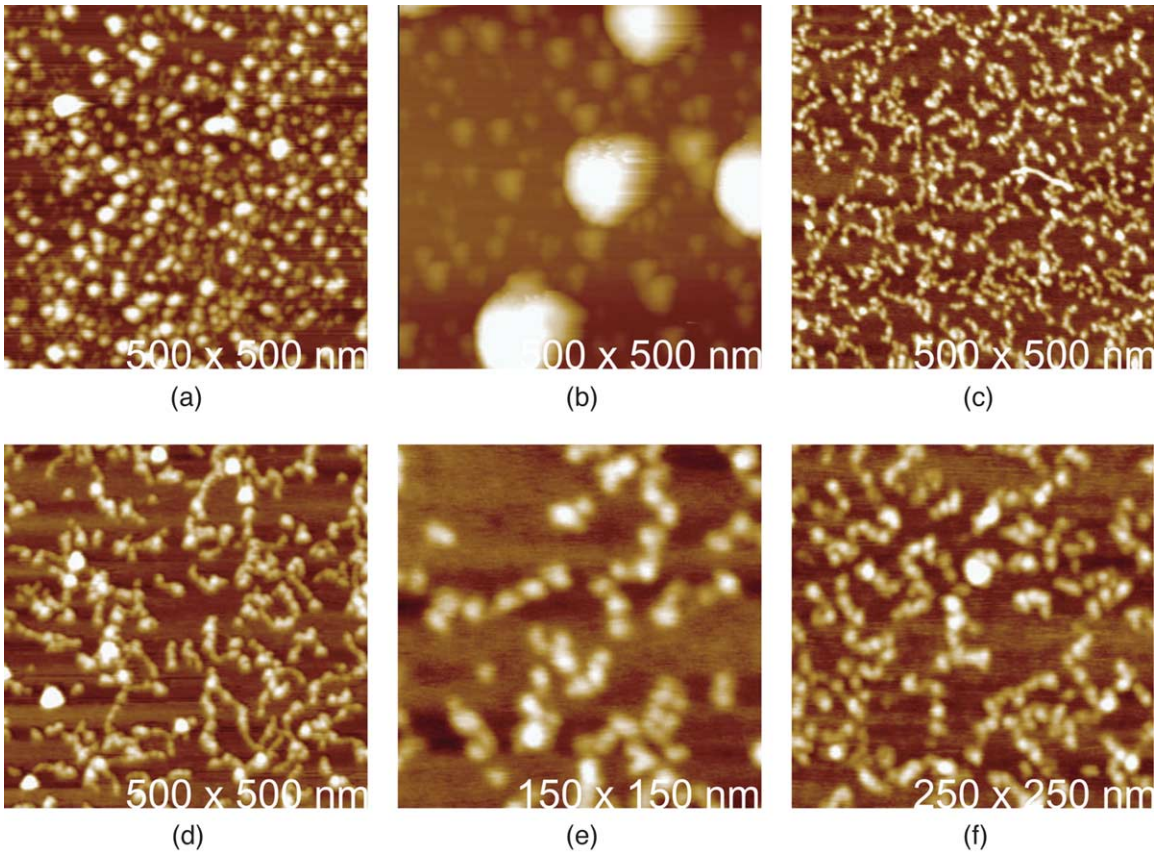

Figure 3. In (a), and at higher magnification in (b), is RNA extracted from STMV. Like poliovirus RNA, it appears as uniform, compact spheres, but of diameter 10 nm, the diameter of the interior of the $T=1$ icosahedral STMV capsid. These spherical particles appear to be stable almost indefinitely at 26 °C. In (c) through (f) are various samples of RNA extracted from STMV after heating to 65 °C. The spheres of RNA transform into chains of structural domains, their lengths reflecting the relative sizes of the genomes. Accordingly, the STMV chains are considerably shorter than the RNAs of the other viruses.

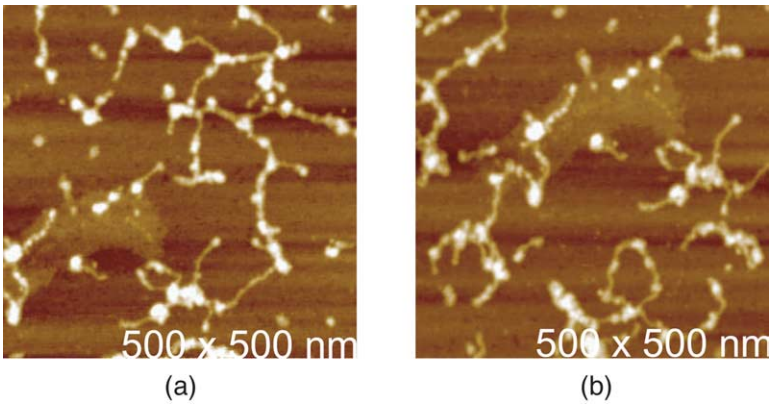

Figure 4. When the STMV RNA is heated further and spread on mica, segments of purely single-stranded RNA are exposed along the chains of domains, and seen to link the domains in a linear manner.

presumably maintained by tertiary interactions, are stable at room temperature.

With heating to 65 °C for 30 minutes, the spherical RNA particles transform, like the RNA from the $T=3$ icosahedral viruses, into chains of discrete densities. As shown in Figure 3(c) through (f), these RNA chains are again segmented into linear arrays of domains, each domain reflecting local secondary structural arrangements. The lengths of the linear assemblies vary up to approximately 100 nm and their thicknesses range from 0.5 nm to 3 nm. The strands of contiguous domains are stable for long periods of time, even at 65 °C. Upon cooling to 4 °C and re-examination by AFM, the fibers revert to uniform spherical particles of 10 nm diameter. Hence, the transformation between uniform spheres and chains of domains is reversible, as it was for poliovirus.

Upon heating to 90–100 °C for several minutes, as illustrated by Figure 4, the chains of domains begin melting into single-stranded threads of height above substrate of 1 nm or less. This parallels what was seen with poliovirus, BMV, and TYMV RNAs, but requires harsher conditions. Once the strands are fully unwound at the elevated temperature, degradation to fragments proceeds.

TMV RNA

RNA extracted from TMV was initially different from RNA extracted from the icosahedral viruses, undoubtedly reflecting its very different mode of encapsidation. Freshly extracted TMV RNA, as seen in Figure 5(a) through (d), appears as long, more or less regular, threads with a height of about 0.5 nm above the substrate. The strands were unlike those

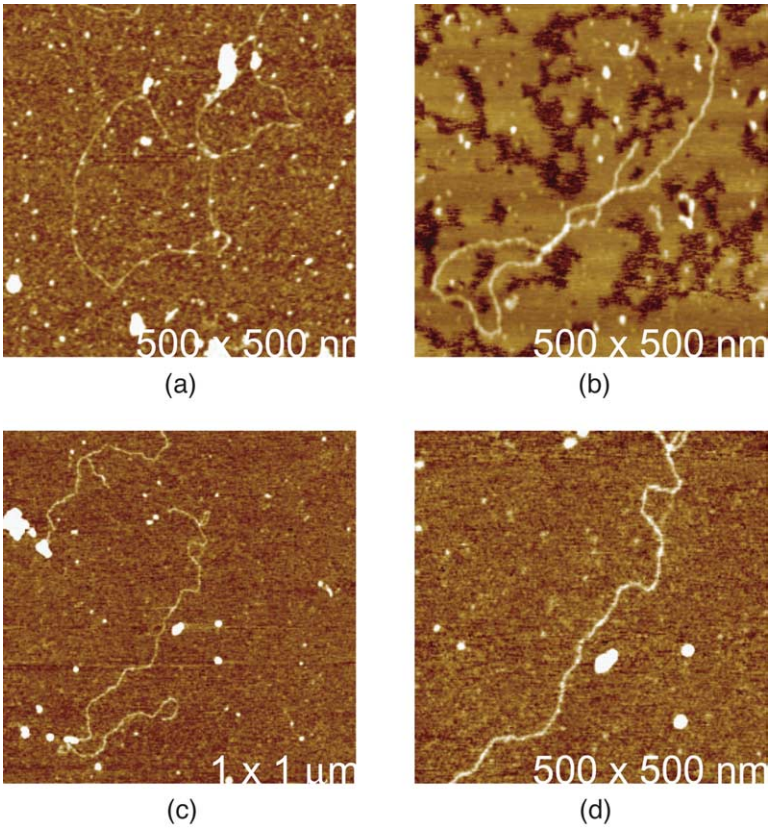

Figure 5. RNA extracted from TMV initially appears as fully unwound single strands arbitrarily disposed on the mica surface. There is no indication of secondary folding units.

from the icosahedral viruses, in that they did not exhibit a distinctive pattern of domains or globular units along their lengths, and only occasionally displayed even one or two such domains. They were simply single strands of RNA appearing to lack secondary structure.

After some time at room temperature, the single strands of RNA transformed gradually into linear arrays of globular domains, like those seen in Figure 6(a) through (c). These closely resembled the segmented fibers of secondary structural units observed for the icosahedral virus RNAs. After several hours, the sequential arrays of domains exhibited by the TMV RNA were virtually indistinguishable from those seen for the RNAs of the icosahedral viruses. If the TMV RNA was subsequently cooled and stored at 4 °C, and re-examined by AFM, it often appeared as thick, highly condensed fibers, like those in Figure 6(d) through (f), large irregular aggregates, and networks of fibers. These, however, were random in size and shape, and distinct from the spherical particles formed by the RNAs of the icosahedral viruses.

If the TMV RNA was exposed to temperatures of 65 °C or more for 15 to 30 minutes, then only single strands of nucleic acid having heights of less than 1 nm were observed on the substrate (data not shown). If the RNAs from any of the viruses were heated above 65 °C for extended periods of time, however, significant degradation occurred and only short fragments of RNA, both with and without secondary structural domains, were observed.

It is noteworthy that in all of our experiments, with all of the RNAs, aggregation of molecules into aggregates and large masses was pervasive. This often made AFM imaging difficult and only with patience could agglutinated masses in some cases be disassociated to reveal their components. These were mixtures of the spherical particles, the chains of secondary domains, and single-stranded threads. RNA is clearly very sticky, and associates rapidly and promiscuously to form tangles and networks.

Discussion

Our AFM images have shown a consistent pattern of structural dynamics by the genomic RNAs extracted from four icosahedral viruses. In each case, the RNA initially exhibited uniform spherical shapes consistent with the interior diameters of the respective virions. This is suggestive, therefore, that the conformation of the RNA immediately after extraction remains that of the encapsidated nucleic acid. This is supported by the

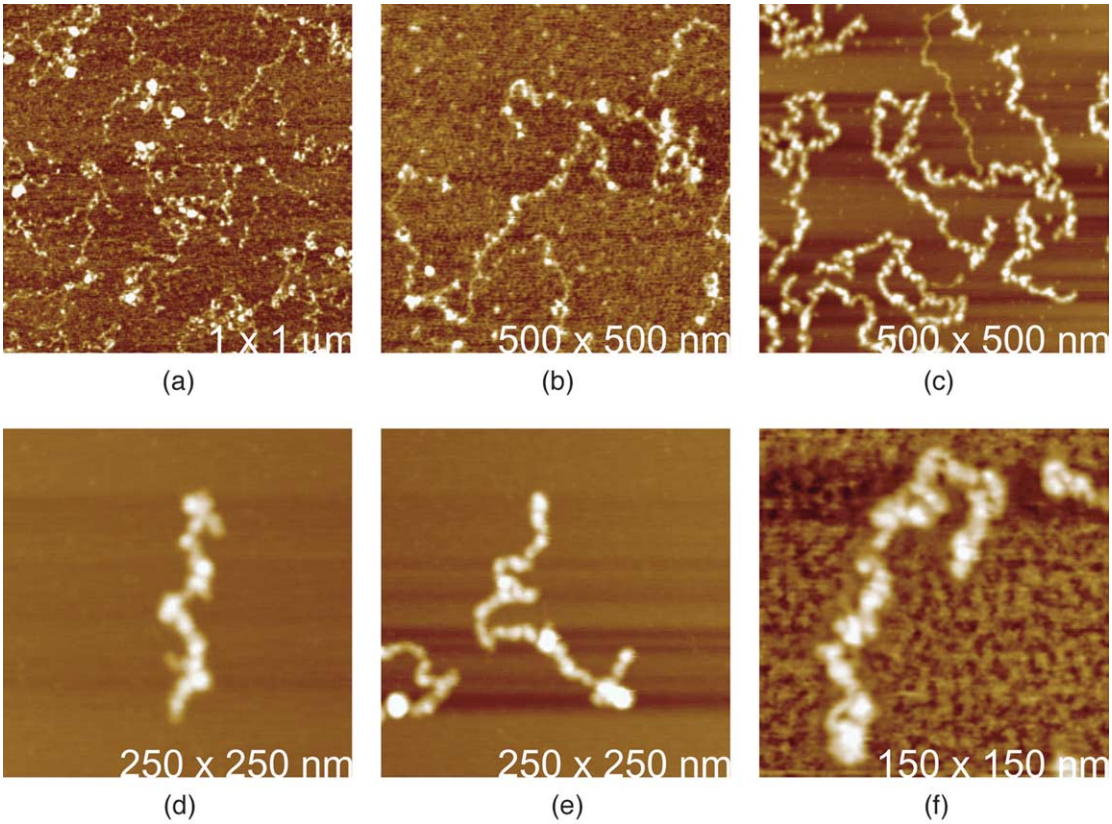

Figure 6. With time in (a) through (c), local secondary folding domains begin to appear spontaneously along the previously extended strands of TMV RNA. They begin to assume the appearance of the RNA extracted from the icosahedral viruses. Ultimately, TMV RNA single strands, in (d) through (f), coalesce into thick fibers of condensed folding domains very similar to those seen in the initial unfolding of icosahedral virus RNA, the transformation of spherical RNA masses into extended chains.

earlier observation that extensive degradation of STMV with proteases yields particles that are indistinguishable from those produced in these experiments by extraction with phenol/chloroform.[39]

Upon heating, or simply being left at room temperature in the case of poliovirus RNA, the nucleic acid lost tertiary interactions and melted into linear arrays of secondary structural elements. It is noteworthy that the folding units, or domains, appeared as a sequential array along single RNA molecules. This implies, that the secondary structures of the RNAs within poliovirus, TYMV, BMV, and STMV exist as series of local folding domains; individual or groups of stem-loops of various sizes and compositions are arranged contiguously. These observations suggest that the secondary structures do not involve long-range pairing interactions, or the formation of long excursions and branches. The same conclusion was reached for TYMV and STMV on the basis of independent considerations.[5,7] The RNA conformations must be, as originally postulated,[40] and supported by others,[33,41–43] a series of local stem-loop structures, and stem-loop superstructures arranged along continuous chains. The results we have obtained here are consistent with such conclusions and illustrate the properties of single-stranded RNA and its dynamics as recently reviewed.[33]

If an internucleotide distance of 6 Å is assumed, then an extended genomic RNA for poliovirus would be 4500 nm, it would be 3790 nm for TYMV, 3800 nm for TMV, and STMV would have an expected extended length of 634 nm. The unfolding of the RNAs from an initial globular form into the chains of domains probably proceeds at different rates for individual molecules. The unfolding is not synchronized. Thus, every molecule in the AFM field of view likely represents a slightly different stage of unfolding. The molecules at any observation time are not of uniform length but exhibit some size distribution.

Nevertheless, we can measure the average end-to-end lengths of the RNA molecules from each virus shortly after they have unfolded from the spherical conformation, but before single-stranded segments become visible, as they are, for example, in Figure 1(b) and (c) for poliovirus, Figure 2(a) and (b) for TYMV, and Figure 3(c) through (f) for STMV. This gives a reasonable estimate of the degree of compaction of the molecules due to the formation of secondary structural domains. The distributions are, in fact, rather narrow, with lengths varying by no more than 10% to 15% about the average. The average end-to-end distances for the genomic RNAs are about 420 nm for poliovirus, 460 nm for TYMV, and 90 nm for STMV. For TMV, where formation of secondary structure occurs with time, the final lengths, like those illustrated in Figure 6(d) through (f) are appropriate, and the average for TMV RNA is 320 nm. BMV RNA was not measured.

The degrees of compaction for the four RNAs are, therefore, 10.7 for poliovirus, 8.2 for TYMV, 7.0 for STMV, and 11.9 for TMV. Since the RNAs of the icosahedral viruses must ultimately be condensed into spheres corresponding to the interior capsid diameter of their respective viruses, it seems evident that formation of tertiary interactions produces a compaction equivalent to or even greater than that due to secondary structural interactions.

The chains of structural domains observed by AFM are reasonably stable, particularly in the case of TYMV and STMV, though significantly less so for BMV. They are disrupted only with heating, vigorous heating in the case of STMV RNA. When melted, however, each RNA reveals its underlying single-stranded RNA composition. Once fully unwound to long single strands lacking secondary structure, the RNAs become susceptible to hydrolysis and are degraded to fragments. Of the RNAs investigated, that from BMV appeared to be the most sensitive to breakdown.

TMV RNA was relevant to these experiments, in that it served, in part, as a negative control. It did not exhibit a spherical, uniform shape upon extraction but appeared as fully extended single strands of RNA. Upon standing, however, it too gradually formed chains of secondary structural domains, qualitatively similar in most respects to the inherent conformations of the RNAs from the icosahedral viruses.

Transitions between the spherical conformation of the RNA and the fibrous, linear chains of secondary structural domains appear to be reversible. This implies that the viral RNA alone, independent of protein, may program its own encapsidated conformation. That is, the primary sequence of the viral RNA may not only code for the proteins necessary for replication, movement, and encapsidation, but also specify the RNA conformation inside the virion. The RNA sequence directs the formation of a chain of distinct secondary structural domains, which in turn forms tertiary interactions that condense the linked domains into spherical masses. The RNA of icosahedral viruses may, in a sense, be a double code. It codes genetically for the proteins and replication signals essential for the virus life-cycle, but equally, it may program the folding of the RNA inside the virion and play a dominant role in directing assembly. The unfolding and refolding *in vitro*, however, is quite slow, requiring 20–40 minutes. It seems probable that *in vivo*, the rate of folding must be much faster, likely accelerated by interaction with the coat protein.

A process that remains unclear from our results, is how, within a living cell, the viral RNA ultimately assumes a fully extended, single-stranded conformation. Indeed, it must do so, otherwise it could not fulfill its physiological roles in RNA replication, movement, and translation. We observe, *in vitro*, that the spherical masses of nucleic acid unfold to reveal a linear array of secondary structural domains. Only under relatively severe conditions, such as heating to 65 °C or beyond, do the chains of

domains of some viruses further unwind to produce single strands. While we can promote full unwinding with temperature, the cell cannot, and it remains a puzzle as to how this comes about. It seems increasingly likely that this may involve RNA melting enzymes.[33]

The strength of the tertiary interactions maintaining the encapsidated conformation in the different viruses varies. Poliovirus unfolds spontaneously into chains of secondary structural domains at room temperature over the period of an hour. The RNA for BMV appears, similarly, to unravel rather quickly, although we have made no quantitative estimates of its transformation. It does, however, also appear to be the most susceptible to degradation. TYMV RNA requires moderate heating to induce it to unravel in a reasonable time. STMV RNA, on the other hand, is very tightly folded into its encapsidated, spherical conformation and requires vigorous heating to 65 °C for 30 minutes or more before tertiary interactions are weakened sufficiently that secondary structural domains are exposed. With further heating, secondary structure melts at the most susceptible points along the chain and segments of single-stranded RNA develop.

The secondary structural domains do not melt out suddenly, as if there were a global and cooperative conformational transition, as is seen for example with double-stranded DNA. The chains melt out at arbitrary points, leaving intact domains separated by single-stranded RNA threads produced by those that have unwound. This is reasonable, since each domain is unique and possesses a specific stability dependent upon its inherent base-pairing capacity and other related features.

The observation that the encapsidated mass of RNA yields a linear array of secondary structural domains that is not branched or present in cruciform or other complex shapes implies that the encapsidated conformation is unlikely to be the minimum energy conformation of the RNA. Secondary domains are connected to one another only by single-stranded threads of RNA, never multiple threads so far as we can see. All minimum energy conformation predictions for single-stranded RNAs that we are aware of involve complex architectures and long-range interactions, and we do not see them. As illustrated most clearly by the TMV RNA, long, single-stranded threads of RNA simply transform into a linear sequence of local folding units that then begin to interact among themselves, again locally but increasingly global, until a high degree of condensation occurs.

The events we witnessed for TMV RNA, where higher-order structure increased consistently, appears the reverse of those observed for the RNAs of the icosahedral viruses. In a sense, they are symmetrical. They likely illustrate the sequence of folding events that pertain for the RNA of icosahedral viruses in attaining their encapsidated conformation.

Materials and Methods

Preparation of viruses

TMV and STMV were harvested simultaneously from the leaves of common tobacco plants (Burley), which were co infected with the viruses. The two viruses were separated by sequential fractionation with polyethylene glycol as described.[44] STMV was further purified by passage through a Sepharose size-exclusion column. Both TMV and STMV were subsequently crystallized, before extraction of RNA, by slow addition of PEG 3350 to 4% w/v (TMV), or dialysis against 25% (w/v) NaCl in water (STMV).

TYMV was prepared from infected Chinese cabbage as described,[45] and further purified by CsCl gradient-centrifugation. Because TYMV loses its RNA upon freezing, it was passed through a 0.22 μm pore size filter and maintained at 4 °C. BMV was prepared from infected barley leaves immediately prior to AFM analysis by conventional procedures.[23] The purity of each of the plant viruses was verified by SDS-PAGE. Intact virions of STMV, TMV, BMV, and TYMV, prior to extraction with phenol/chloroform, were also spread on substrates and imaged to confirm their homogeneity. Their appearances have been reported elsewhere.[23,39,46,47] Poliovirus was prepared from infected HeLa cells grown to a density of 1.2×10^9 cells/l. The final purification was by centrifugation on 15%–30% (w/v) sucrose gradients at 24 °C for 2.5 hours at 28,000 rpm in a Beckman SW28 swinging bucket rotor.[48]

Extraction of RNA

Fractions of the sucrose gradients containing poliovirus were extracted twice with a mixture of 50% (v/v) phenol, 50% (v/v) chloroform, and back-extracted with the same. Aqueous phases were precipitated with 2.5 volumes of ethanol. After one hour at −20 °C the fractions were centrifuged at 4 °C for ten minutes at 10,000 rpm. RNA pellets were washed with 5 ml of 70% (v/v) ethanol, dried, and resuspended in 200 μl of diethylpyrocarbonate (DEPC)-treated water. Precipitation and washing with ethanol was repeated and the final RNA pellet was resuspended in 100 μl of DEPC-treated water and stored at −70 °C. The concentration of the RNA was determined by measuring absorbance and ranged from 1 μg/μl to 2 μg/μl for poliovirus, and 4 μg/μl or more for the plant viruses (see below). Homogeneity of the RNA was confirmed by agarose gel electrophoresis. The RNA from poliovirus, along with that from STMV prepared in the same manner, was translated *in vitro* using [^{35}S]methionine and shown to produce the expected protein products following SDS-PAGE (data not shown).

The RNAs from the four plant viruses were prepared in the same way as was done for poliovirus, except the viruses themselves were purified by separate procedures appropriate to the specific virus (see above). RNA homogeneity was confirmed by agarose gel electrophoresis and by *in vitro* translation of RNA in the case of STMV. The final RNA samples were dissolved in DEPC-treated water.

Some experiments were carried out on RNAs from the plant viruses to investigate the effects of ions. In the presence of EDTA and monovalent cations up to concentrations of 5 mM and 50 mM, respectively, no change in the appearance of the RNA by AFM was observed. The presence of divalent cations, such as Mg^{2+} or Ni^{2+}, however, clearly produced marked aggregation

of the nucleic acid that made imaging of single RNA molecules virtually impossible. The divalent cation-induced condensation of the RNA was not readily reversible, at least using moderate procedures. Precipitation by ethanol or propanol appeared to have no affect on RNA structure that was perceptible by AFM.

Because of the unusual stability of the STMV capsids, an alternative procedure was used that involved digestion of the capsid for 45 minutes at 65 °C with proteinase K at a protease to virus ratio of 1 : 4 (w/w). This was followed immediately by extraction with phenol/chloroform as described above. Digestion with proteinase K did not affect the RNA as judged by light-scattering,[39] gel electrophoresis, and examination by AFM, but did increase yield of RNA significantly.

AFM procedures

The choice of substrate for AFM visualization of RNA was investigated at length. Single-stranded RNA did not adhere reproducibly to untreated mica. In addition, single-stranded threads of RNA lacking secondary structure rise above the substrate plane no more than 0.5 nm to 1 nm. Therefore, the substrates had to be extremely flat and smooth. RNA adhered well to poly-L-lysine-coated mica, but the poly-L-lysine created an irregular, locally variable surface topology that made imaging problematic. RNA also adhered to mica treated with $NiCl_2$, but this promoted aggregation of the nucleic acid in most instances. The most consistent results were obtained by pre-treating mica surfaces using a silenizing agent.[49,50] This substrate surface proved acceptably smooth for imaging and RNA usually adhered. RNA specimens were diluted appropriately into DEPC-treated water and drops were placed onto the treated mica surfaces. After several minutes the excess liquid was shaken off, the substrate rinsed once with a drop of water and then dried in a stream of dry nitrogen.

Specimens were mounted conventionally with double-sided tape on the J-piezoscanner of a Nanoscope IIIa atomic force microscope (Digital Instruments, Santa Barbara, CA). Silicon RTESP cantilevers were used, and imaging was carried out in air. The images were collected in tapping mode[51,52] at frequencies of about 300 kHz. The forces were similar to those employed in earlier studies on viruses[46,53,54] and biological crystals.[55–57]

There is considerable previous AFM work concerning double-stranded DNA[49,58,59] but, with some exceptions,[58,60–62] rather little on single-stranded RNA. Before investigating single-stranded RNA, DNA plasmids pET19B (Sigma Biochemical Co. St. Louis, MO) were spread on mica and imaged. Plasmid double-stranded DNA posed little problem and images were recorded that were comparable to those in the literature. DNA adhered more readily to a variety of substrates, and rose more than 2 nm above the substrate surface.

Acknowledgements

This research was supported by NIH grants GM58868-02 (A.M.) and AI22693 (B.S.). The authors thank Mr Aaron Greenwood for assistance in preparing the Figures.

References

1. Johnson, J. E. & Rueckert, R. R. (1997). Packaging and release of the viral genome. In *Structural Biology of Viruses* (Chin, W., Burnett, R. M. & Garcea, R., eds), pp. 269–287, Oxford University Press, Oxford.
2. Kaper, J. M. (1975). The chemical basis of virus structure, dissociation and reassembly. *Front. Biol.* **39**, 1–485.
3. Larson, S. B., Koszelak, S., Day, J., Greenwood, A., Dodds, J. A. & McPherson, A. (1993). Three-dimensional structure of satellite tobacco mosaic virus at 2.9 Å resolution. *J. Mol. Biol.* **231**, 375–391.
4. Larson, S. B., Day, J., Greenwood, A. & McPherson, A. (1998). Refined structure of satellite tobacco mosaic virus at 1.8 Å resolution. *J. Mol. Biol.* **277**, 37–59.
5. Hellendoorn, K., Mat, A. W., Gultyaev, A. P. & Pleij, C. W. (1996). Secondary structure model of the coat protein gene of turnip yellow mosaic virus RNA: long, C-rich, single-stranded regions. *Virology*, **224**, 43–54.
6. Hellendoorn, K. (1996). Folding and coat protein binding of tymovirus RNA. PhD thesis, University of Leiden.
7. Larson, S. B. & McPherson, A. (2001). Satellite tobacco mosaic virus RNA: structure and implications for assembly. *Curr. Opin. Struct. Biol.* **11**, 59–65.
8. Larson, S. B., Koszelak, S., Day, J., Greenwood, A., Dodds, J. A. & McPherson, A. (1993). Double helical RNA in satellite tobacco mosaic virus. *Nature*, **361**, 179–182.
9. Larson, S. B., Koszelak, S., Day, J., Greenwood, A., Dodds, J. A. & McPherson, A. (1993). The three-dimensional structure of satellite tobacco mosaic virus at 2.9 Å resolution. *J. Mol. Biol.* **231**, 375–391.
10. Chen, Z. G., Stauffacher, C., Li, Y., Schmidt, T., Bomu, W., Kamer, G. *et al.* (1989). Protein-RNA interactions in an icosahedral virus at 3.0 Å resolution. *Science*, **245**, 154–159.
11. Larson, S. B., Lucas, R. W. & McPherson, A. (2005). Crystallographic structure of the $T=1$ particle of brome mosaic virus. *J. Mol. Biol*. In the press.
12. Fisher, A. J. & Johnson, J. E. (1993). Ordered duplex RNA controls capsid architecture in an icosahedral animal virus. *Nature*, **361**, 176–179.
13. Binning, G., Quate, C. F. & Gerber, C. (1986). Atomic force microscope. *Phys. Rev. Letters*, **56**, 930–933.
14. Bustamante, C. & Keller, D. (1995). Scanning force microscopy in biology. *Phys. Today*, **48**, 32–38.
15. Wimmer, E., Hellen, C. U. & Cao, X. (1993). Genetics of poliovirus. *Annu. Rev. Genet.* **27**, 353–436.
16. Racaniello, V. R. (2001). Picornaviridae: the viruses and their replication. In *Fields Virology* (Knipe, D. M. & Howley, P. M., eds), vol. 1, pp. 685–722, Lippincott Williams and Wilkins, Philadelphia, PA.
17. Semler, B. L. & Wimmer, E. (2002). Editors of *Molecular Biology of Picornaviruses*, American Society for Microbiology Press, Washington, DC.
18. Morch, M. D., Boyer, J. C. & Haenni, A. L. (1988). Overlapping open reading frames revealed by complete nucleotide sequencing of turnip yellow mosaic virus genomic RNA. *Nucl. Acids Res.* **16**, 6157–6173.
19. Canady, M. A., Larson, S. B., Day, J. & McPherson, A. (1996). Crystal structure of turnip yellow mosaic virus. *Nature Struct. Biol.* **3**, 771–781.
20. Hirth, L. & Givord, L. (1988). Tymoviruses. In *The Plant Viruses* (Koenig, R., ed.), pp. 163–212, Plenum Press, New York.

21. Lane, L. C. (1977). Brome mosaic virus. *CMI/AAB Descript. Plant Viruses*, **180**, 1–4.
22. Ahlquist, P., Allison, R., Dejong, W., Janda, M., Kroner, P., Pacha, R. & Traynor, P. (1990). Molecular biology of bromovirus replication and host specificity. In *Viral Genes and Plant Pathogenesis* (Pirone, T. P. & Shaw, J. G., eds), pp. 144–155, Springer, New York.
23. Lucas, R. W., Kuznetsov, Y. G., Larson, S. B. & McPherson, A. (2001). Crystallization of brome mosaic virus (BMV) and $T=1$ brome mosaic virus particles following a structural transition. *Virology*, **286**, 290–303.
24. Mirkov, T. E., Mathews, D. M., Du Plessis, D. H. & Dodds, J. A. (1989). Nucleotide sequence and translation of satellite tobacco mosaic virus RNA. *Virology*, **170**, 139–146.
25. Valverde, R. A. & Dodds, J. A. (1986). Evidence for a satellite RNA associated naturally with the U5 strain and experimentally with the U1 strain of TMV. *J. Gen. Virol.* **67**, 1875–1884.
26. Valverde, R. A. & Dodds, J. A. (1987). Some properties of isometric virus particles which contain the satellite RNA of TMV. *J. Gen. Virol.* **68**, 965–972.
27. Ban, N., Larson, S. B. & McPherson, A. (1995). Structural comparison of the plant satellite viruses. *Virology*, **214**, 571–583.
28. Matthews, R. E. F. (1981). *Plant Virology* (2nd edit.), Academic Press, New York.
29. Holmes, K. C. (1984). The structure determination of tobacco mosaic virus. In *Biological Macroolecules and Assemblies* (Jurnak, F. A. & McPherson, A., eds), vol. 1, pp. 121–148, Wiley, New York.
30. Stubbs, G. (1984). Macromolecular interactions. In *Tobacco Mosaic Virus* (Jurnak, F. A. & McPherson, A., eds), pp. 149–202, Wiley, New York.
31. Bloomer, A. C. & Butler, P. J. G. (1986). Tobacco mosaic virus: structure and self-assembly. In *The Plant Viruses* (Regenmortel, M. H. V. V. & Fraenkel-Courat, H., eds), pp. 19–52, Plenum Press, New York.
32. Hogle, J. M., Chow, M. & Filman, D. J. (1985). Three-dimensional structure of poliovirus at 2.9 Å resolution. *Science*, **229**, 1358–1365.
33. Onoa, B. & Tinoco, I., Jr (2004). RNA folding and unfolding. *Curr. Opin. Struct. Biol.* **14**, 374–379.
34. Turner, D. H. (2000). Conformational changes. In *Nucleic Acids: Structure, Properties and Functions* (Bloomfield, V., Crowthers, D. & Tinoco, I., eds), pp. 259–334, University Science Books, Mill Valley, CA.
35. Caspar, D. L. D. & Klug, A. (1962). Physical principles in the construction of regular viruses. *Cold Spring Harbor Symp. Quant. Biol.* **27**, 1–24.
36. Kitamura, N., Semler, B. L., Rothberg, P. G., Larsen, G. R., Adler, C. J., Dorner, A. J. *et al*. (1981). Primary structure, gene organization and polypeptide expression of poliovirus RNA. *Nature*, **294**, 547–553.
37. Dasgupta, R., Alhlquist, P. & Kaesberg, P. (1980). Sequence of the 3′ untranslated region of brome mosaic virus coat protein messenger RNA. *Virology*, **104**, 339–346.
38. Dasgupta, R. & Kaesberg, P. (1982). Complete nucleotide sequences of the coat protein messenger RNAs of brome mosaic virus and cowpea chlorotic mottle virus. *Nucl. Acids Res.* **10**, 703–713.
39. Day, J., Kuznetsov, Y. G., Larson, S. B., Greenwood, A. & McPherson, A. (2001). Biophysical studies on the RNA cores of satellite tobacco mosaic virus. *Biophys. J.* **80**, 2364–2371.
40. Fresco, J. R., Alberts, B. M. & Doty, P. (1960). Some molecular details of the secondary structure of ribonucleic acid. *Nature*, **188**, 98–101.
41. Spirin, A. S. (1963). Some problems concerning the macromolecular structure of ribonucleic acids. *Prog. Nucl. Acid Res.* **1**, 301–345.
42. Witz, J. & Strazielle, C. (1973). Viral RNAs. In *Subunits in Biological Systems, part B* (Fasman, G. D. & Timasheff, S. N., eds), Marcel Dekker, New York.
43. Murthy, V. L. & Rose, G. D. (2003). RNABase: an annotated database of RNA structures. *Nucl. Acids Res.* **31**, 502–504.
44. Koszelak, S., Dodds, J. A. & McPherson, A. (1989). Preliminary analysis of crystals of satellite tobacco mosaic virus (STMV). *J. Mol. Biol.* **209**, 323–326.
45. Canady, M. A., Day, J. & McPherson, A. (1995). Preliminary X-ray diffraction analysis of crystals of turnip yellow mosaic virus (TYMV). *Proteins: Struct. Funct. Genet.* **21**, 78–81.
46. Kuznetsov, Y. G., Malkin, A. J., Lucas, R. W., Plomp, M. & McPherson, A. (2001). Imaging of viruses by atomic force microscopy. *J. Gen. Virol.* **82**, 2025–2034.
47. Malkin, A. J., Kuznetsov, Y. G., Lucas, R. W. & McPherson, A. (1999). Surface processes in the crystallization of turnip yellow mosaic virus visualized by atomic force microscopy. *J. Struct. Biol.* **127**, 35–43.
48. Harris, T. J., Dunn, J. J. & Wimmer, E. (1978). Identification of specific fragments containing the 5′ end of poliovirus RNA after ribonuclease III digestion. *Nucl. Acids Res.* **5**, 4039–4054.
49. Lindsay, S. M., Tao, N. J., DeRose, J. A., Oden, P. I., Lyubchenko Yu, L., Harrington, R. E. & Shlyakhtenko, L. (1992). Potentiostatic deposition of DNA for scanning probe microscopy. *Biophys. J.* **61**, 1570–1584.
50. Zuccheri, G. & Samori, B. (2002). Methods in cell biology. In *Atomic Force Microscopy in Cell Biology* (Jena, B. P., ed.), vol. 68, pp. 713–720, Academic Press, New York.
51. Hansma, H. G. & Hoh, J. H. (1994). Biomolecular imaging with the atomic force microscope. *Annu. Rev. Biophys. Biomol. Struct.* **23**, 115–139.
52. Hansma, H. G., Browne, K. A., Bezanilla, M. & Bruice, T. C. (1994). Bending and straightening of DNA induced by the same ligand: characterization with the atomic force microscope. *Biochemistry*, **33**, 8436–8441.
53. Kuznetsov, Y. G., Victoria, J. G., Robinson, W. E., Jr & McPherson, A. (2003). Atomic force microscopy investigation of human immunodeficiency virus (HIV) and HIV-infected lymphocytes. *J. Virol.* **77**, 11896–11909.
54. Kuznetsov, Y. G., Datta, S., Kothari, N. H., Greenwood, A., Fan, H. & McPherson, A. (2002). Atomic force microscopy investigation of fibroblasts infected with wild-type and mutant murine leukemia virus (MuLV). *Biophys. J.* **83**, 3665–3674.
55. McPherson, A., Malkin, A. J., Kuznetsov, Y. G. & Plomp, M. (2001). Atomic force microscopy applications in macromolecular crystallography. *Acta Crystallog. Sect. D*, **57**, 1053–1060.
56. McPherson, A., Malkin, A. J. & Kuznetsov, Yu. G. (2000). Atomic force microscopy in the study of macromolecular crystal growth. *Annu. Rev. Biophys. Biomol. Struct.* **29**, 361–410.
57. Kuznetsov, Yu. G., Malkin, A. J., Land, T. A., DeYoreo, J. J., Barba, A. P., Konnert, J. & McPherson, A. (1997).

Molecular resolution imaging of macromolecular crystals by atomic force microscopy. *Biophys. J.* **72**, 2357–2364.
58. Hansma, H. G., Kasuya, K. & Oroudjev, E. (2004). Atomic force microscopy imaging and pulling of nucleic acids. *Curr. Opin. Struct. Biol.* **14**, 380–385.
59. Shlyakhtenko, L. S., Miloseska, L., Potaman, V. N., Sinden, R. R. & Lyubchenko, Y. L. (2003). Inter-segmental interactions in supercoiled DNA: atomic force microscope study. *Ultramicroscopy*, **97**, 263–270.
60. Bonin, M., Zhu, R., Klaue, Y., Oberstrass, J., Oesterschulze, E. & Nellen, W. (2002). Analysis of RNA flexibility by scanning force spectroscopy. *Nucl. Acids Res.* **30**, e81.
61. Hansma, H. G., Oroudjev, E., Baudrey, S. & Jaeger, L. (2003). TectoRNA and "kissing-loop" RNA: atomic force microscopy of self-assembling RNA structures. *J. Microsc.* **212**, 273–279.
62. Williams, M. C. & Rouzina, I. (2002). Force spectroscopy of single DNA and RNA molecules. *Curr. Opin. Struct. Biol.* **12**, 330–336.

Edited by J. Doudna

(Received 12 October 2004; received in revised form 17 December 2004; accepted 2 January 2005)